| | |
|---|---|
| **Citation/Reference** | Borbála Hunyadi, Aleksandra Siekierska, Jo Sourbron, Daniëlle Copmans, Peter AM de Witte (2017),<br>**Automated analysis of brain activity for seizure detection in zebrafish models of epilepsy**<br>Journal of Neuroscience Methods, vol. 287, pp 13-24 |
| **Archived version** | Author manuscript: the content is identical to the content of the published paper, but without the final typesetting by the publisher |
| **Published version** | http://www.sciencedirect.com/science/article/pii/S0165027017301516?via%3Dihub |
| **Journal homepage** | https://www.journals.elsevier.com/journal-of-neuroscience-methods |
| **Author contact** | borbala.hunyadi@esat.kuleuven.be<br>*+ 32 (0)16 321799* |
| **IR** | https://lirias.kuleuven.be/handle/ |

*(article begins on next page)*

# Automated analysis of brain activity for seizure detection in zebrafish models of epilepsy

Borbála Hunyadi[1,2], Aleksandra Siekierska[3], Jo Sourbron[3], Daniëlle Copmans[3] and Peter A.M. de Witte[3]

[1]STADIUS Center for Dynamical Systems, Signal Processing and Data Analytics, Department of Electrical Engineering (ESAT), KU Leuven, Kasteelpark Arenberg 10, 3001 Leuven, Belgium
[2]iMinds Medical IT, Leuven, Belgium
[3]Laboratory for Molecular Biodiscovery, KU Leuven, Campus Gasthuisberg, Herestraat 49, O&N II, 3000 Leuven, Belgium

Keywords: local field potential (LFP), epilepsy, zebrafish larvae, animal model, seizure detection, automated analysis, SVM, classification, machine learning

## Abstract

Background. Epilepsy is a chronic neurological condition, with over 30% of cases unresponsive to treatment. Zebrafish larvae show great potential to serve as an animal model of epilepsy in drug discovery. Thanks to their high fecundity and relatively low cost, they are amenable to high-throughput screening. However, the assessment of seizure occurrences in zebrafish larvae remains a bottleneck, as visual analysis is subjective and time-consuming.

New method. For the first time, we present an automated algorithm to detect epileptic discharges in single-channel local field potential (LFP) recordings in zebrafish. First, candidate seizure segments are selected based on their energy and length. Afterwards, discriminative features are extracted from each segment. Using a labeled dataset, a support vector machine (SVM) classifier is trained to learn an optimal feature mapping. Finally, this SVM classifier is used to detect seizure segments in new signals.

Results. We tested the proposed algorithm both in a chemically-induced seizure model and a genetic epilepsy model. In both cases, the algorithm delivered similar results to visual analysis and found a significant difference in number of seizures between the epileptic and control group.

Comparison with Existing Methods. Direct comparison with multichannel techniques or methods developed for different animal models is not feasible. Nevertheless, a literature review shows that our algorithm outperforms state-of-the-art techniques in terms of accuracy, precision and specificity, while maintaining a reasonable sensitivity.

Conclusion. Our seizure detection system is a generic, time-saving and objective method to analyze zebrafish LPF, which can replace visual analysis and facilitate true high-throughput studies.

## 1. Introduction

Epilepsy is a collective term for a wide spectrum of neurological disorders, characterized by sudden, recurrent seizure episodes. Seizures may cause various kinds of severe clinical symptoms, loss of consciousness, injury, and even death. In approximately one third [1] of the 65 million cases worldwide [2], the

occurrence of seizures cannot be controlled with anticonvulsant drugs. These patients continue to have seizures and consequently experience a serious negative impact on their quality of life. Therefore, there are continued efforts towards developing better medications to treat epilepsy.

Zebrafish models of epilepsy are gaining popularity in drug discovery research. Their small size, high fecundity and optical transparency enable easy observation under basic stereomicroscope and high-throughput screening [3]. Moreover, the close homology of their genome to the human one makes them an appropriate model for studying pathophysiology of human epilepsies. Different genetic manipulations [4] as well as various chemical treatment options [5] can be applied to induce epilepsy or epileptic seizure-like behavior in zebrafish larvae in order to model different aspects and subtypes of epilepsy.

Common to all epilepsies, seizures occur due to an abnormal, excessive and synchronous activity of large neuronal populations. As such, seizures can be observed on electrophysiological recordings such as invasive or non-invasive local field potential (LFP) measurements, being a counterpart of electroencephalogram (EEG) performed in humans. Indeed, these techniques serve as a gold standard for epilepsy diagnosis. In the current context, LFP recordings for monitoring seizure activity can be used to validate novel zebrafish epilepsy models, as well as to evaluate the efficacy of new drug candidates.

Manual analysis of EEG/LFP recordings is time-consuming and prone to subjectivity. Alternatively, automated analysis techniques can save time and provide an objective assessment of seizure occurrences. Although the electrical patterns generated during an epileptic seizure in humans, rodents and zebrafish can be described by very similar dynamical models and share some fundamental characteristics [6], they are observed at very different spatiotemporal scales. Seizure patterns and brain activity of different sources appear different depending on the recording equipment (e.g. invasive or non-invasive) due to volume conduction. Finally, equipment as well as recording conditions determine the types of artifact and noise superimposed on brain signals. Therefore, existing seizure detection algorithms cannot be applied directly; nevertheless, some of their features can be adapted to the current problem.

Automated human epileptic seizure detection algorithms have a very extensive literature, the first published works dating back to the early ‘80s [7]. Typical algorithms start with a feature extraction step, where the EEG is characterized by certain linear or non-linear metrics in the time, frequency or time-frequency domain, on the level of the EEG channels or extracted sources [8] [9]. Subsequently, automated decision is made based on calculated features using criteria such as knowledge-based rules, neural networks or other classification techniques [10]. Due to the fact that seizure patterns of different patient groups and even individual patients can be very different, algorithms are dedicated either to adults [11] or neonatal patients [12], or work in a patient-specific manner [13]. The use of automated seizure detection techniques in animal models of epilepsy is scarce, although a few promising approaches to detect seizures on intracranial recordings in rodents have been published [14] [15]. Recently, a long-term, non-invasive platform for electrophysiological monitoring of zebrafish larva [16] was introduced, including an automated seizure monitoring option. To our knowledge, this is the only existing automated LPF scoring system developed for zebrafish larvae to date. One of the two main

features of the algorithm is based on measuring the correlation among the multichannel electrode signals. Considering that many electrophysiological recording systems measure a single channel, this approach is not widely applicable.

We propose a novel seizure detection algorithm based on single-channel LFP recorded from zebrafish larva. Different zebrafish models of epilepsy can produce seizures with very different length, morphology, and occurrence rate. Therefore, it is challenging to develop an algorithm, which can reliably detect seizures from various models. We propose a universal pipeline based on a preselection of candidate events, a discriminative feature set and machine learning. A model-specific classifier is automatically trained by feeding training LFP data from a specific model to the learning machine, which will be suitable to detect seizures from the same epilepsy model. We illustrate the applicability of our proposed method for a chemically-induced seizure model and a genetic epilepsy model, i.e. respectively the convulsant pentylenetetrazole (PTZ) and the homozygous *scn1Lab* mutant [17]. However, after applying proper training data, this approach can also be used on any other model.

In section 2.1 we discuss our measurement setup and the LFP datasets, which were used in this study. Then, in section 2.2 we present the criteria and the protocol for manual labeling of the data based on visual analysis, and the characteristics of typical events observed in LFP recordings. In section 2.3 we explain the technical details of the proposed seizure detection algorithm, while section 2.4 presents the metrics used to evaluate the performance of our technique. In section 2.5 we discuss the possibility to manually adapt the seizure detection system if necessary. Subsequently, our results are presented; regarding the outcome of the manual labeling (section 3.1), the optimal algorithmic choices based on the training data (section 3.2); and the final results obtained on the test data (sections 3.3). Finally, section 4 is dedicated to the critical discussion of our study.

# 2. Materials and Methods

## 2.1. Data collection

### 2.1.1. Zebrafish husbandry

Adult zebrafish (*Danio rerio*) of the AB strain were maintained at 28.5 °C on a 14-h light/10-h dark cycle under standard aquaculture conditions, and fertilized eggs were collected via natural spawning. Embryos were raised in Danieau's medium (1.5 mM HEPES, pH 7.6, 17.4 mM NaCl, 0.21 mM KCl, 0.12 mM $MgSO_4$ and 0.18 mM $Ca(NO_3)_2$) in an incubator on a 14-h light/10-h dark cycle at 28.5 °C. All zebrafish experiments were approved by the Ethics Committee of the University of Leuven (Ethische Commissie van de KU Leuven, approval number 061/2013 and 154/2015) and by the Belgian Federal Department of Public Health, Food Safety and Environment (Federale Overheidsdienst Volksgezondheid, Veiligheid van de Voedselketen en Leefmileu, approval number LA1210199).

### 2.1.2. Chemically-induced seizure model and genetic epilepsy models in zebrafish

1. Chemical model

7 dpf wild-type zebrafish larvae (AB) were incubated 2 hours with 1% DMSO in a 100 µl volume of Danieau's medium, whereafter either 100 µl of Danieau's medium (hereafter referred to as VHC group), or 100 µl of 40 mM PTZ (hereafter referred to as PTZ group) was added for 15 minutes to obtain a 20 mM working concentration.

2. Genetic models

Two different genetic models were used: 5 dpf morpholino (MO)-injected larvae (transient knockdown of a previously validated epilepsy-causing gene [18]) and 7 dpf *scn1Lab* mutant zebrafish larvae (having point mutation M1208R leading to a loss-of-function of the *nav1.1Lb* channel [19]). Hereafter we refer to the wild-type and homozygote larvae as WT group and HO group, respectively.

### 2.1.3. Local field potential (LFP) recordings

1. Invasive LFPs

For invasive LFP recordings a patch pipette was inserted into the optic tectum or forebrain of a larva immobilized in 2% low melting point agarose (Invitrogen). A recording electrode was filled with ACSF and connected to a high-impedance amplifier. Subsequently, recordings were performed for 10 minutes in current clamp mode, band pass filtered at 0.1-1000 Hz, digital gain 10, at sampling intervals of 10 µs (MultiClamp 700B amplifier, Digidata 1440A digitizer, both Axon instruments, USA).

2. Non-invasive LFPs

Non-invasive recordings, where the electric signal is read from the skin of larva's head, were performed as described previously [20]. The recording electrode (borosilicate soda-glass pipet, GC150TF-7.5, Harvard Apparatus, UK) was pulled with a DMZ Universal Puller (Zeitz, Germany) to a diameter of approximately 20 microns and filled with artificial cerebrospinal fluid (ACSF, 124 mM, NaCl, 2 mM KCl, 2 mM $MgSO_4$, 2 mM $CaCl_2$, 1.25 mM $KH_2PO_4$, 26 mM $NaHCO_3$ and 10 mM glucose). The larva was immobilized in 2% low melting point agarose (Invitrogen). The differential signal between the recording electrode positioned on larva's head above the optic tectum or forebrain and the reference electrode was amplified 10,000 times by DAGAN 2400 amplifier (Minnesota, USA), band pass filtered at 0.3-300 Hz and digitized at 2 kHz via a PCI-6251 interface (National Instruments, UK) with WinEDR (John Dempster, University of Strathclyde, UK). The duration of each recording was 10 minutes.

### 2.1.4. Training and test data sets

1. Chemical model

Training data were obtained from non-invasive LFPs consisting of recordings from 15 VHC and 15 PTZ larvae. Test data were obtained from non-invasive LFPs consisting of recordings from 20 VHC and 20 PTZ larvae.

2. Genetic models

Training data were obtained from invasive LFPs consisting of recordings from 31 MO-injected larvae. Test data were obtained from non-invasive LFPs consisting of recordings from 20 WT and 20 HO larvae.

### 2.2. Manual detection

All training and test recordings were reviewed and epileptic events were manually labeled using Clampfit 10.2 (Molecular Device Corporation, USA) by experienced LFP experts (A.S., J.S. or D.C.). The following criteria were applied to classify an electrical discharge as a positive LFP event: (i) the amplitude equal to at least three times the amplitude of the baseline, (ii) regular polyspike pattern with at least three spikes, and (iii) a duration of at least 50 ms (genetic model, test data), 60 ms (genetic model, training data) or 100 ms (chemical model). For the chemical model two subsequent events were considered as one if the distance between them was less than 200 ms. Such a cut-off value was not necessary in the genetic model, where the events were clearly distinct.

It is often difficult to visually differentiate epileptic discharges from artifacts, impeding an objective decision. Therefore, high amplitude events were labeled as one of the following three classes: ‘epileptic’, ‘artifact’ or ‘dubious’. Figure 1 shows a 10 s long segment of LFP with four high-amplitude events, recorded in a zebrafish larva (genetic model) in the training dataset. Observing the events on smaller time scales reveals a regular polyspike pattern in case of event A and B, which were marked as ‘epileptic’ that is, fulfilling all previously mentioned criteria for a positive LFP event. Event C was categorized as ‘dubious’, due to the irregular nature of the discharges making its classification difficult. Event D was marked as an ‘artifact’, because it lacked the typical polyspiking pattern. A typical artifact is slower and less sharp than an epileptic spike, and it can result from a twitch or movement.

Figure 2 shows a 20 s long segment of LFP recorded in a PTZ-treated zebrafish larva (chemical model) in the training dataset. The segment contains two typical events characteristic for the PTZ model: a ‘high-amplitude’ seizure (Figure 2 A) and a ‘low-amplitude’ event (Figure 2 B), with a small amplitude, but showing a polyspike pattern. Besides these characteristic events the chemical models also produce ‘generic’ seizures similar to those spotted in other models.

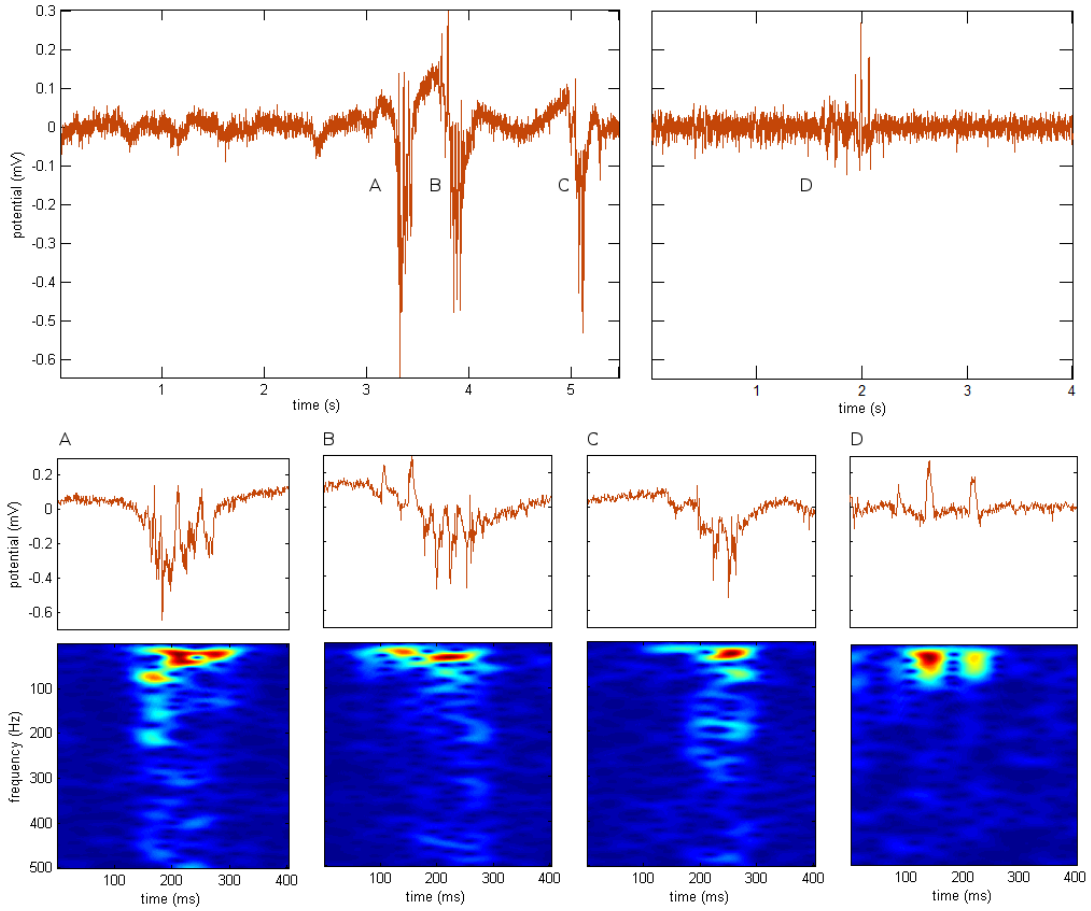


*Figure 1: An example of a non-invasive LFP segment with events labeled as 'epileptic' (A and B), 'dubious' (C) and 'artifact' (D) representative for the genetic model in the training dataset (top panel). Magnification of these events together with their corresponding time-frequency maps (obtained by short-time Fourier transform) is shown in the bottom panel.*

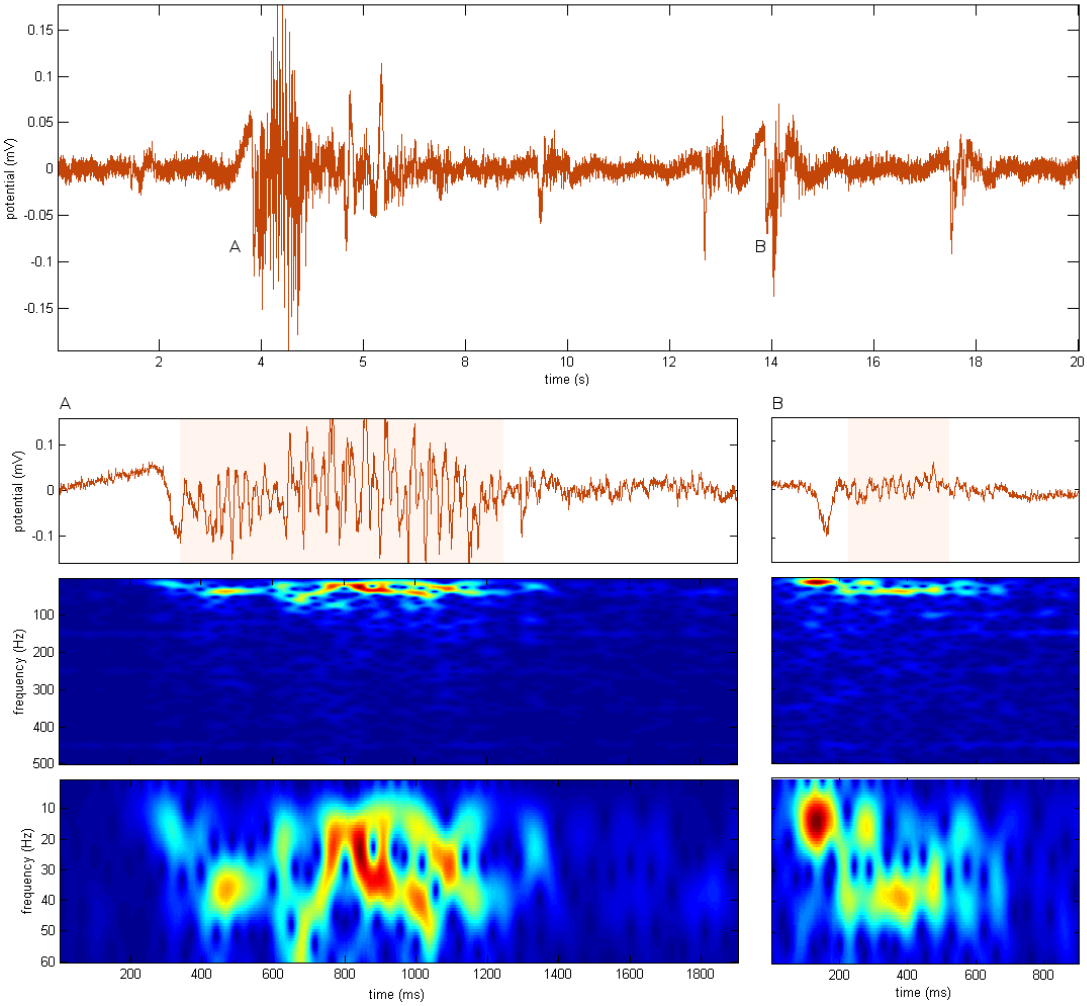


*Figure 2: An example of an LFP segment with events labeled as 'high-amplitude' (A) and 'low-amplitude' (B) typical for the PTZ model (top panel). Magnification of these events together with their corresponding time-frequency maps is shown in the bottom panel. The time-frequency map is shown both for broad band (0-500Hz) and for a narrower band (0-60Hz). The total seizure duration is indicated by the shaded area in the magnified time domain signals.*

### 2.3. Automated detection

Figure 3 summarizes the consecutive steps of the training and testing of the automated seizure detection algorithm. First, the labeled training data was preprocessed (step 1). Then, events (i.e. LFP signal segments), which stand out from the baseline were selected as seizure candidates (step 2). Afterwards, a set of features was computed on the segments (step 3). These features were used to train the classifier (step 4). Steps 2-4 were repeated several times using different parameters at step 2 and using different machine learning methods to train the classifier at step 4. The best parameters and best machine learning solution were chosen by evaluating each combination in a leave-one-recording-out cross-validation setting (step 5). Finally, using the selected parameters and machine learning solution, a final classifier was trained using all available training data. Below each step is explained in detail.

Step 1. Preprocessing. EEG data were downsampled to 1 kHz. EEG samples with abnormally high potential (>1mV) were linearly interpolated using the neighboring samples. Then, the signals were high-pass filtered with a 6$^{th}$ order Butterworth filter. In case of the genetic model (recorded with the invasive equipment) the cut-off frequency was set at 1Hz. However, we observed unexplained low-frequency fluctuation in some of the initially inspected data (not part of the datasets used in the study) recorded with the non-invasive equipment. Therefore, non-invasively recorded data was filtered with a cut-off of 10Hz. Finally, the time series was normalized to zero mean and unit standard deviation.

Step 2. Event selection. The non-linear energy operator (NLEO) [12] was applied on the normalized time series:

$$\psi(x_n) = x_{n-l} \cdot x_{n-p} - x_{n-q} \cdot x_{n-s}$$
$$with\ l = 1, p = 2, q = 0, s = 3$$

The advantage of the NLEO over other energy operators is the fact that its value is proportional to the square of both the amplitude and the frequency of the signal. Therefore, it enhances high-amplitude high-frequency activity compared to background. Then, a threshold $\tau_{NLEO}$ was applied on the resulting time series. Suprathreshold samples, which were less than 20 ms (200 ms for chemical models) apart, were grouped together in one segment. Finally, segments, which were longer than a threshold $\tau_{len}$, were retained as candidate seizure events.

Step 3. Feature extraction. A number of time and frequency domain features, which are widely used in the literature, were extracted from each candidate segment. Time domain features include absolute maximum amplitude, root mean square amplitude, the number of zeros, minima and maxima of the segment, as well as the mean and the standard deviation of the length of the intervals in between consecutive zero crossings. Frequency domain features were computed from the continuous wavelet transform of the signal using morlet wavelets at scales equivalent to frequencies between 10-100 Hz (chemical model) and 2-100 Hz (genetic model), with 1 Hz resolution. The difference in the frequency range for the two types of models was due to the different preprocessing (see above at Step 1.) The upper limit of 100 Hz was determined based on examining the spectrogram (Figure 2, bottom panels) of epileptic discharges of representative examples in the training dataset. Then, the average wavelet power coefficient over the whole segment at each scale was taken, resulting in 91 and 99 features for the chemical and the genetic model, respectively. Furthermore, the average power at 11-20, 21-50 and 51-100 Hz sub-bands (chemical model) or 1-10, 1-20, 1-50 and 1-100Hz (genetic model) were also computed. For the genetic model two final frequency domain features were computed as the ratio between the average power in low frequency band (1-10 Hz and 1-20 Hz) and average broad band (1-100 Hz). These feature was specifically designed to characterize movement artifacts, based on the observation that sudden transient movements of the larva caused high amplitude spike-like waveforms on the EEG at frequencies in the lower frequency bands. However, due to the higher, 10 Hz cut-off frequency filtering in the non-invasively recorded data, these features were not extracted from the

chemical model data. As a result, a total of 101 and 112 features were extracted from the chemical and the genetic model data, respectively.

Step 4. Training. The feature vectors extracted from each candidate event, along with their class labels, were fed to different machine learning algorithms to train a classifier. Note that for the genetic model only events in the 'epileptic' and 'artifact' classes were used for training; 'dubious' events were discarded. For the chemical model all epileptic events, including 'generic', 'high-amplitude' and 'low-amplitude' were used for training. The following machine learning solutions were investigated:

a. K-nearest neighbor classifier with k={5,11,21} [21]
The K-nearest neighbor is a simple but effective method to classify a new sample or observation $x \in \mathbb{R}^d$, described by d number of features, based on a training dataset $\{x_n,y_n\}$, n=1,…,N, with $x_n \in \mathbb{R}^d$ training samples and $y_n=\{-1,1\}$ class labels. The classifier works as follows. First, the distances between the new sample and all training samples are computed. Here we used the Euclidian distance:

$$d_n = (x - x_n)(x - x_n)'$$

Then, the distances $d_n$ are sorted in ascending order, and the K training samples with the smallest distances from the new sample are selected. Finally, the class membership of the new sample $x$ is determined by majority voting based on the class labels of the selected training samples.

b. Support vector machines (SVM) with linear or radial basis function (RBF) kernel [22]
A SVM classifier learns an optimal separating hyperplane based on a training dataset $\{x_n,y_n\}$, n=1,…,N, with $x_n \in \mathbb{R}^d$ training samples and $y_n=\{-1,1\}$ class labels. In our case the training samples are the feature vectors extracted from each epoch and the class labels indicate whether an epoch is a seizure or not. The classifier makes decisions based on the following formula:

$$y(x) = sign[w^T\varphi(x) + b]$$

Here, $w$ is a weighting vector and $\varphi$ is a (non-linear) function mapping the input data to a higher dimensional feature space. The SVM aims to construct a separating hyperplane in the feature space with maximal margin:

$$\min_{w,e_n b} \frac{1}{2} w^T w + C \sum_{n=1}^{N} e_n$$

subject to

$$y_n[w^T\varphi(x) + b] \geq 1 - e_n, e_n \geq 0, n = 1, \dots, N$$

In the above optimization problem C is a regularization constant, also called the box constraint. The dual problem can be formulated by taking the Lagrangian and the conditions for optimality, leading to the following quadratic programming problem:

$$\max_{\alpha} \sum_{n=1}^{N} \alpha_n - \sum_{n=1}^{N} \sum_{m=1}^{N} \alpha_n \alpha_m y_n y_m K(x_n x_m)$$

subject to

$$\sum_{n=1}^{N} \alpha_n y_n = 0 \; and \; 0 \leq \alpha_n \leq C \; for \; n = 1, \ldots, N$$

The function $K(x_n,x_m)$ is a symmetric and positive definite kernel function that satisfies the Mercer theorem. The $x_n$ input vectors which correspond to a non-zero $\alpha_n$ values are the so-called support vectors. The classifier in the dual space takes the form:

$$y(x) = sign[\alpha_n y_n K(x, x_n) + b]$$

c. Least-squares support vector machine (LS-SVM) with linear or RBF kernel [23]

In the LS-SVM formulation, a squared loss function and equality constraints are used instead of inequality constraints in (2):

$$\min_{w,e_n b} \frac{1}{2} w^T w + \gamma \sum_{n=1}^{N} {e^2}_n$$

subject to

$$y_n[w^T \varphi(x) + b] = 1 - e_n.$$

This simplifies the computation to the solving a set of linear equations instead of the original quadratic programming problem:

$$\begin{bmatrix} 0 & y^T \\ Y & \Omega + \gamma^{-1} I \end{bmatrix} \begin{bmatrix} b \\ \alpha \end{bmatrix} = \begin{bmatrix} 0 \\ 1_N \end{bmatrix}$$

with $y=[y_1, \ldots, y_N]^T$, $1_N=[1, \ldots, 1]^T$, $e=[e_1, \ldots, e_N]^T$, $\alpha=[\alpha_1, \ldots, \alpha_N]^T$, and $\Omega_{n,m}= y_n y_m K(x_n,x_m)$.

Step 5. Evaluation. Many different classifiers were trained by repeating steps 2-4 for all possible combinations of machine learning approaches and the following different parameters: $\tau_{NLEO}$ = {5, 10, 15, 20, 25, 30} and $\tau_{len}$ = {50, 60, 70, 80, 90, 100}. The performance of the classifiers was evaluated based on their positive predictive value (PPV, also known as selectivity or precision):

$$PPV = \frac{number \; of \; true \; positives}{number \; of \; true \; positives + number \; of \; false \; positives}$$

The higher the PPV, the more likely it is that a detected segment is a true seizure. The PPV of each classifier was evaluated in a leave-one-recording-out cross-validation setting, where all but one EEG recordings were used for training and the remaining EEG recording was used for testing. After this procedure was repeated for each recording, the average PPV value was taken. The best possible combination of parameters and machine learning solution (including the tuning of the SVM hyperparameters) was selected based on the cross-validated PPV value

In the final training phase candidate events were selected using the optimal parameters from all available training EEG recordings and, after feature extraction the final classifier was trained. Again, this step included the tuning of the SVM hyperparameters using a grid search over a logarithmic grid in the leave-one-recording-out cross-validation setting.

In the test phase the EEG data was preprocessed, candidate events were selected using the optimal parameters, the same features were extracted and these features were then fed to the classifier, created in the final training phase.

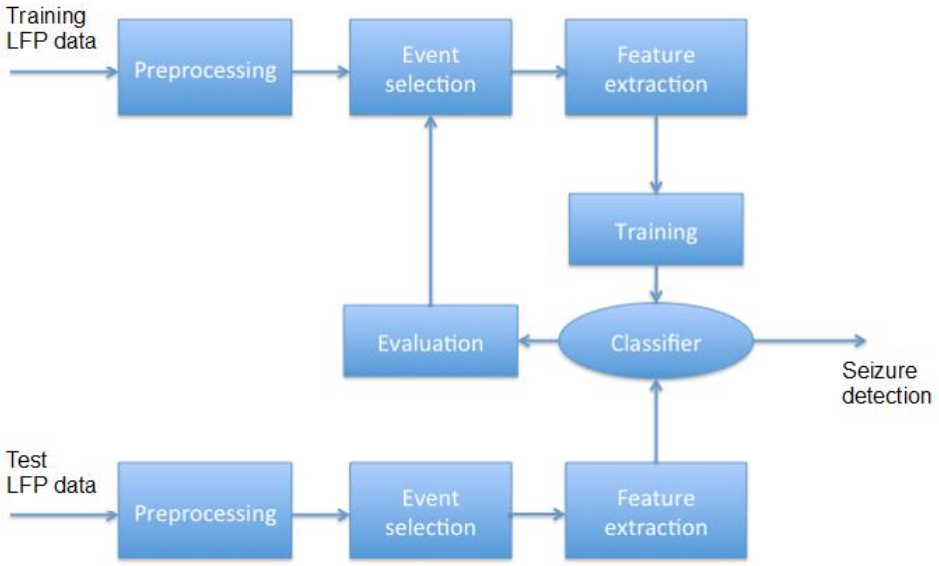


*Figure 3: Overview of the automated analysis method: consecutive steps for training the optimal classifier on a labeled training set and detecting seizures in an unknown test set.*

### 2.3. Performance metrics

The performance of automated seizure detection was evaluated in comparison with the outcome of the manual detection in terms of the following 3 measures:

- frequency of the epileptiform discharges, defined as the number of occurrences per 10 minute recording
- cumulative duration of the epileptiform discharges in a 10 minute recording
- number of seizing larvae, defined as the number of larvae with at least three seizures

All test datasets (both chemical and genetic models) consisted of two groups, one where seizures were expected to occur (respectively PTZ and HO group) and one where no seizures were expected to occur (respectively VHC and WT group).

Using the three measures explained above, we have evaluated whether the automated analysis delivers similar results to manual analysis, as well as whether it reliably quantifies the difference between the two groups in each test dataset. Statistical comparisons were made using Wilcoxon's matched-pairs signed rank tests (comparison of frequency and cumulative duration of seizure detected manually or automatically), Mann-Whitney tests (comparison of frequency and cumulative duration of seizures between different groups) or Fisher's exact test (contingency table of seizing / non-seizing larvae).

In addition, to facilitate comparison with other methods in the literature, we also calculated the following commonly used performance metrics for those datasets where seizures are expected to occur (i.e. the PTZ and HO groups):

$$Sensitivity = \frac{TP}{(TP + FN)}$$

$$Specificity = \frac{TN}{(TN + FP)}$$

$$Positive\ predictive\ value\ (PPV) = \frac{TP}{(TP + FP)}$$

$$Accuracy = \frac{TP + TN}{(TP + FP + FN + TN)}$$

$$False\ positives\ per\ seizure\ (FPPS) = \frac{FP}{TP + FN}$$

$$False\ negatives\ per\ seizure\ (FNPS) = \frac{FN}{TP + FN}$$

Where TP, TN, FP and FN mean the number of true positive, true negative, false positive and false negative detections, respectively. Some of these numbers are easily calculated as the number of correctly detected seizures (TP), number of missed seizures (FN), or the number of times the algorithm makes a false detection (FP). However, the number of true negatives cannot be defined in a straight-forward way in our case. Our algorithm works on the basis of events, where the length of the event is determined in a data-driven way and may vary. In contrast, many algorithms in the literature work on the basis of fixed length epochs, therefore, they can easily count the number of epochs without a seizure. In order to estimate the number of false negatives, we mimicked this approach and divided our test data to 1 s long epochs. We consider those epochs to be true negatives, which do not contain any samples of a manually or an automatically detected seizure.

### 2.4. Adaptability

The age, convulsant and genotype of zebrafish larvae, as well as recording equipment and conditions may influence the characteristics of the epileptic discharges, artifacts and baseline of the LFPs. Therefore, a classifier trained in a certain dataset may not be optimal when any of the above circumstances change. However, it is time consuming and impractical to collect and manually analyze a new training dataset each time. Therefore, our proposed solution allows some adaptability without the need of retraining. Namely, if necessary, the $\tau_{len}$ and $\tau_{NLEO}$ parameters can be adapted at the testing phase. This will affect the set of candidate events. The rest of the algorithm is not modified, i.e. the previously trained classifier is used to select the epileptic discharges from the altered pool of candidate events. To tune the $\tau_{len}$ and $\tau_{NLEO}$ parameters, a small subset of the test data can be used, which is manually analyzed. Then, the parameters can be adjusted until the automated detection approximates the results of visual judgement at a satisfactory level.

# 3. Results

## 3.1. Manual analysis of training data

Manual analysis of a single 10 minute long recording takes, on average, an estimated 20 minutes. Below we report the number and the cumulative duration of the events marked that served as training.

In the chemical model, PTZ-treated larvae had a total of 580 seizures (38,7 per subject ± 34,5 standard deviation), while VHC-treated larvae had a total of 13 seizures (0,9 ± 2,1). The average duration of PTZ- and VHC-treated larvae was 874 ms and 287 ms, resulting in a cumulative duration of 613,9s (40,9s ± 39,5) and 4,5s (0.3s ± 0.8), respectively.

In the genetic model, a total of 1051 events were marked, among which 519 (on average 16,7 per subject ± 10,9 standard deviation, same notation used further below) as 'seizure', 385 (12,4 ± 7,9) as 'artifact' and 147 (4,7 ± 4,2) as 'dubious'. The average duration of a seizure was 101,4 ms, resulting in a total cumulative duration of 52,7s (1757,4 ms ± 1104,3). Clearly, the chemical model produced more and longer seizures than the genetic model used in this study, which motivated us to train different classifiers for the different models. Moreover, as expected, there is a large difference between the number and cumulative duration of the seizures in the PTZ- and VHC-treated larvae.

## 3.2. Optimal parameters and classifier

As explained in the methods section, many classifiers were trained using all combinations of possible machine learning techniques, different $\tau_{NLEO}$ and $\tau_{len}$ parameters for both the chemical and genetic models separately. The classifiers were evaluated in a leave-one-recording-out cross-validation setting on the training data and the optimal classifier was selected based on the cross-validated PPV. The results are presented below for each model separately.

### 3.2.1. Chemical model

For the chemical model, PPV was computed considering all detections in the PTZ group as true positives, and all detections in the VHC group as false positives.

Figure 4 shows the PPV obtained by different classifiers at different $\tau_{NLEO}$ and $\tau_{len}$ parameter values. In general, there seems to be an increasing trend in PPV for increasing $\tau_{NLEO}$ and $\tau_{len}$ for all classifiers, except for support vector machines with linear kernel. Interestingly, this technique outperformed all other classifiers for nearly all combinations of $\tau_{NLEO}$ and $\tau_{len}$ parameters. Overall, the best results were achieved by support vector machines with a linear kernel at $\tau_{NLEO}$=20. Using these choices, the final classifier was retrained using all training data of chemical model larvae, and the box-constraint parameter C was optimized in a leave-one-recording-out cross-validation setting over a vector of logarithmically spaced points. The optimal value (C=2.71) was selected based on the lowest misclassification error rate.

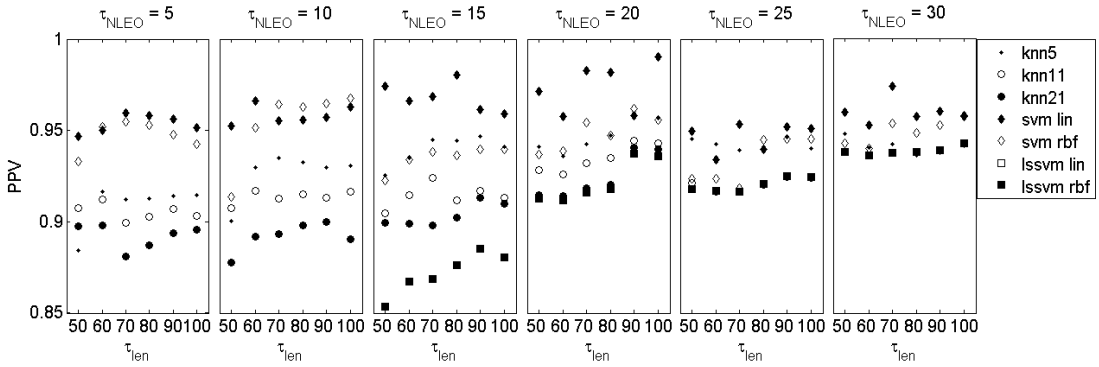


*Figure 4: Selection of the best classifier and optimal parameters for the chemical model: cross-validated positive predictive value (PPV) of different classifiers at different $\tau_{NLEO}$ parameters on the training data. For $\tau_{NLEO}$ = {5, 10} PPV of* lssvm rbf *is below 0.85, therefore, it does not appear on the graphs. Abbreviations:* knn5, knn11 and knn21 *- k-nearest neighbor classifiers with k=5, k=11 and k=21,* respectively*;* svm lin, svm rbf, lssvm lin *and* lssvm rbf *- support vector machine and least-squares support vector machine with linear and RBF kernel).*

### 3.2.2. Genetic model

For the genetic model, PPV was computed considering all detected 'epileptic' events as true positives, and all detected 'artifacts' as false positives. Events labeled as 'dubious' and detected by the algorithm were not considered either true or false positives. According to the definition of epileptic discharges used for manual detection, 2 different length threshold parameters were evaluated, i.e. $\tau_{len}$={50, 60}. As shown on the first two graphs of Figure 5, regardless of the $\tau_{NLEO}$ and $\tau_{len}$ parameters, linear support vector machine (SVM) classifiers perform the best of all machine learning techniques, followed tightly by SVM with RBF kernel and k-nearest neighbor classifiers. Increasing both $\tau_{len}$ and $\tau_{NLEO}$ leads to small improvement in PPV, but the differences above $\tau_{NLEO}$ = 20 are minor. Therefore, the sensitivity of the classifiers was also investigated, shown in the last two graphs in Figure 5. With increasing $\tau_{NLEO}$, sensitivity decreases considerably in a sharper trend at $\tau_{len}$ = 60 than at $\tau_{len}$ = 50. Note that regarding sensitivity, the SVM with RBF kernel slightly outperforms linear SVM. Although there is no clear winner combination, $\tau_{len}$ = 50 and $\tau_{NELO}$ = 20 was chosen to train the final support vector machine classifier with a RBF kernel using all training data of the genetic model.

Using these choices, the final classifier was retrained using all training data of genetic model larvae, and the box-constraint parameter C and kernel scale σ were optimized in a leave-one-recording-out cross-validation setting over a grid of logarithmically spaced points. The optimal values (C=1 and σ=7,38) were selected based on the lowest misclassification error rate.

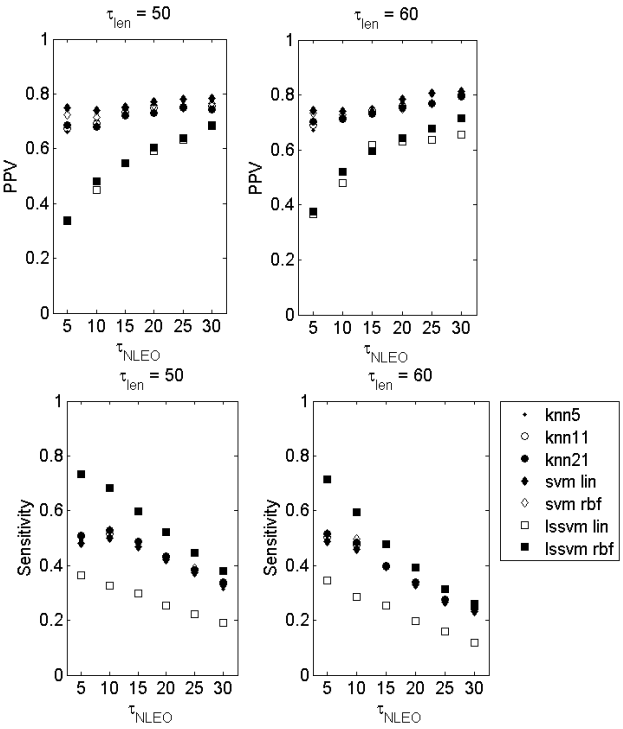


*Figure 5: Selection of the best classifier and optimal parameters for the genetic model: cross-validated positive predictive value (PPV) and sensitivity of different classifiers at different $\tau_{NLEO}$ and $\tau_{len}$ parameters on the training data. Abbreviations:* knn5, knn11 and knn21 *- k-nearest neighbor classifiers with k=5, k=11 and k=21,* respectively*;* svm lin, svm rbf, lssvm lin *and* lssvm rbf *- support vector machine and least-squares support vector machine with linear and RBF kernel).*

### 3.2.3 Discriminative power of features

The discriminative power of the extracted features were investigated using a Kruskal-Wallis test. The null hypothesis of this non-parametric test states that the values in the two groups (seizure and non-seizure in our case) come from distributions with equal medians. Therefore, a rejection of the hypothesis (sufficiently small p-value) means that the distributions have different medians, i.e. the features are discriminative for the different groups. Feature comparisons were made after pre-selection of candidate segments using the optimal $\tau_{NLEO}$ and $\tau_{len}$ determined above. The results are shown in Figure 6.

The time domain features (number of zero crossing, minima and maxima; and the average interval length between zero crossings) are significantly discriminative for both zebrafish models at $p<0.05$. Many of the frequency domain features are also strongly discriminative in both models ($p<0.2$). For the chemical model, strongly discriminative features include the Morlet wavelet powers between 11-20Hz, 30-75Hz, and 89-100Hz. The average power between 11-20 and 21-50Hz are significantly discriminative. For the genetic model, the discriminative power of individual Morlet wavelet powers fluctuates a lot across the 2-100 band. However, the average power in 1-20Hz band, 1-100 band and the ratio between low frequency band and broad band (1-20Hz vs 1-100Hz) are significant at $p<0.05$. Note that this analysis is on a feature by feature basis. A combination of certain features might have a good discriminative power even in case they are individually not very powerful.

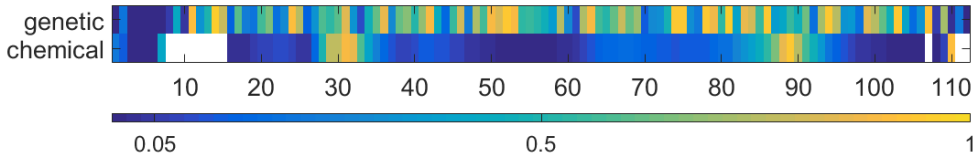


*Figure 6: Discriminative power of the features in the genetic and chemical models. The features are organized along the x axis in the following order: 1: absolute maximum amplitude 2: root mean square amplitude 3-5: number of zero crossings, minima and maxima of the segment 6-7: mean and the standard deviation of the length of the intervals in between consecutive zero crossings 8-106: wavelet power at each scale 107-110: average power in 1-10, 1-20, 1-50 and 1-100Hz band (genetic) and average power in 11-20, 21-50 and 51-100Hz band (chemical; no entry for feature nr. 107) 111-112: power ratio between low and broad band (1-10 vs 1-100 and 1-20 vs 1-100Hz). Features which were not extracted for the chemical model (see 2.3 for more explanation) are indicated in white. Dark blue color means that a feature is significantly different across the seizure and non-seizure segments.*

### 3.3. Seizure detection performance in test data

#### 3.3.1. Chemical model

Figure 7 shows the comparison between the results obtained by manual and automated seizure analysis. On average, manual and automated analysis detected respectively 23,7 ± 10,3 and 23,0 ± 12,4 seizures per larvae in the PTZ group (p=0,39), which is significantly higher (p<0.001 with both analysis methods) than 1,2 ± 1,8 and 1,7 ± 2,3 (p=0,12) in the VHC group. Similarly, there is a significant difference between the groups in terms of cumulative duration of the seizures: 28060 ms ± 14422 in PTZ and 321 ms ± 550 in VHC using manual detection (p<0.001), and 12252 ms ± 6507 in PTZ and 550 ms ± 806 in VHC (p<0.001) using automated detection. Note that automated analysis sometimes detects only a few short segments of a single long seizure event in PTZ. This is reflected in a significantly shorter cumulative duration for automated analysis than for manual detection (p<0.001). Besides, some manually marked events were missed by the automated analysis. These were typically seizures which are shorter than average (<1000 ms). Overall, both manual and automated analysis found 19 out of 20 seizing larvae in the PTZ group, significantly more than in the VHC group (p<0.001 for both analysis methods). In the VHC group manual and automated analysis found 3 and 6 seizing larvae, respectively. This difference is not significant (p=0.45). In summary, automated analysis can reliably distinguish the PTZ and VHC groups.

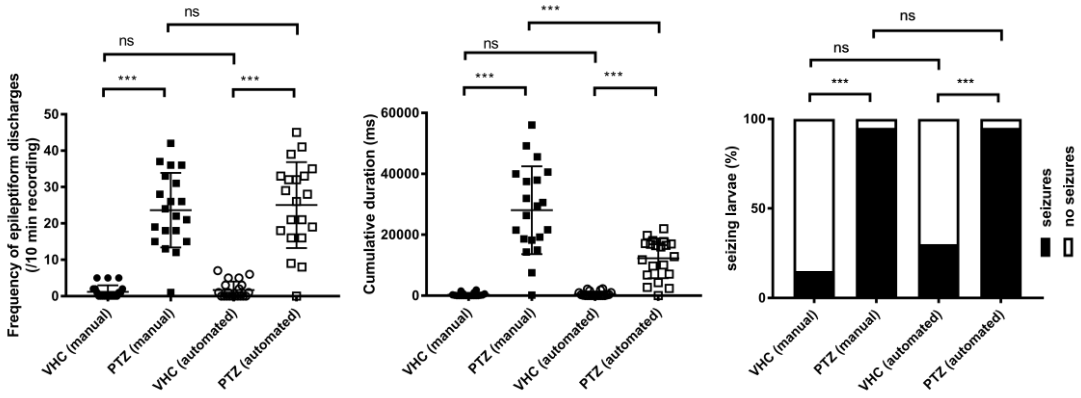


*Figure 7: Comparison between the manual and automated seizure detection in the chemical model. Notation: ns - no significant difference; *** - p < 0.001.*

### 3.3.2. Genetic model

The results obtained for the genetic model zebrafish larvae show very similar trends as for the chemical model. As shown in Figure 8, manual and automated analysis detected respectively 7,3 ± 3,8 and 6,9 ± 4,2 seizures per larvae in the HO group (p=0,78), which is significantly higher (p<0.001 with both analysis methods) than 0,7 ± 1,0 and 0,7 ± 1,2 (p>0.99) in the WT group. Similarly, there is a significant difference between the groups in terms of cumulative duration of the seizures: 1653ms ± 1376 in HO and 89ms ± 225 in WT using manual detection (p<0.001), and 675ms ± 490 in HO and 66ms ± 136 in WT (p<0.001) using automated detection. However, similarly as for the chemical model, the cumulative duration of epileptic events detected automatically is significantly shorter than detected manually (p<0,001). Overall, 19 and 18 seizing larvae were found in the HO group by manual and automated analysis, respectively, while both analysis methods found two seizing larvae in the WT group. In summary, automated analysis can reliably distinguish the HO and WT groups.

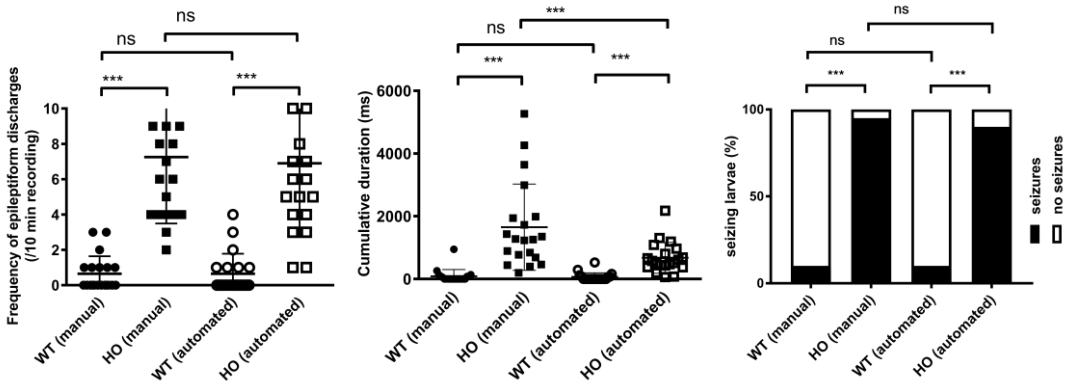


*Figure 8: Comparison between the manual and automated seizure detection trained on the invasively recorded and tested on the non-invasively recorded genetic group. Notation: ns - no significant difference; *** - p < 0.001.*

### 3.3.3. Adaptability

We have explored whether the results can be improved by adjusting the $\tau_{NLEO}$ parameter for selecting candidate events in the genetic model's test data (but using the same classifier specified in section 3.3.2. and 3.3.3., i.e. the ones trained with the previously set threshold).

The automated analyses detected events and with a shorter cumulative duration than manual analysis. Therefore, we gradually lowered the threshold in order to achieve a less stringent event selection, i.e. a higher sensitivity. Using $\tau_{NLEO}$=15, the performance of the algorithm improved: at this setting the cumulative duration of the events detected by the algorithm was comparable to the results of the manual analysis, as shown in Figure 9. Choosing a lower $\tau_{NLEO}$ has produced too many false detections both in the HO and the WT group (not shown).

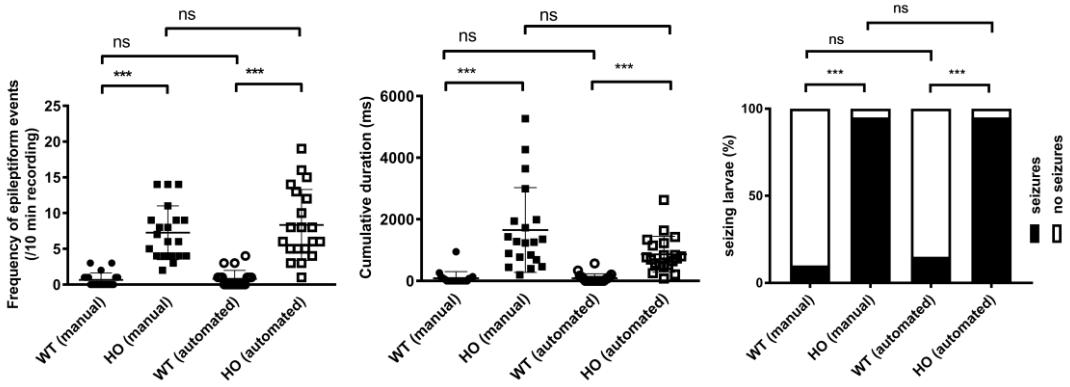


*Figure 9: Comparison between the manual and automated seizure detection in the genetic model. The automated algorithm was trained with $\tau_{NLEO}$=20 and tested on the independent test set with $\tau_{NLEO}$=10. Notation: ns - no significant difference; *** - p < 0.001.*

### 3.3.4. Comparison with literature

Direct comparison of the performance of the proposed method with that of previous approaches in the literature is difficult, as each study uses different datasets and different performance metrics. Unfortunately, no seizure detection performance has been reported using the zebrafish monitoring platform [16]. Nevertheless, we provide a rough comparison with various seizure detection approaches reported in rodent studies since 2013. We excluded those studies that preselect artifact-free EEG segments, or make use of patient (subject)-specific training. Furthermore, we did not select studies, which aim to detect absence seizures, as such seizures typically manifest in very consistent spike-wave patterns in the EEG. They are usually detected with higher accuracy than other seizure types [24], and can be efficiently recognized using dedicated wavelet-based strategies [25].

The results are summarized in Table 1. In general, our method achieved higher accuracy, precision and specificity than the state-of-the-art, however, at the cost of a lower sensitivity. Note that the algorithm presented in [14] detects three different events, namely spikes, seizures and abnormal events, which is a more difficult task than detecting seizure alone. The authors also report performance metrics for spike and seizure detection only, reaching 99% accuracy and 91% specificity, which is similar to the performance of our approach. Note, however, that the parameters used in the detection algorithm in

this study as well as in [26] were fine-tuned on the test dataset itself, as opposed to our study. Finally, the algorithm based on reservoir computing [24] combines an exceptionally high number of true detections (sensitivity and FNPS outperforms our approach) with a low number of false positives (FPPS) comparable to our performance, and a slightly lower specificity. Although this study used a disjoint training and test set, different seizures from the same rats were included in both sets. As intra-subject consistency of seizures may be higher than the inter-subject consistency, this may positively influence the performance metrics reported.

*Table 1: A comparison in performance of the proposed algorithm with various methods from the literature. Sensitivity, specificity, precision and accuracy are reported in the literature as epoch-based measures, while false positives per seizure is an event-based measure. Note that where possible, we report both event- and epoch-based metrics (in brackets). Abbreviations: n.a. – not applicable.*

| Model | Sensitivity | Specificity | Precision | Accuracy | FPPS | FNPS |
|---|---|---|---|---|---|---|
| Chemical | 72% (60.6%) | 99.7% | 91.4% (94.9%) | 96% | 0.08 | 0.29 |
| Genetic | 73.9% (70.8%) | 99.8% | 85.7% (78.0%) | 99.4% | 0.13 | 0.22 |
| [14] (spike / seizure) | 78% / 77% | 90% / 83% | 63% | 87% | n.a. | n.a. |
| [25] | 83% | 95% | n.a. | n.a | n.a. | n.a. |
| [23] | 95.8% | 98.1% | n.a. | n.a. | 0.13 | 0.01 |
| | | | | | | |

3.3.5. Implementation

The proposed seizure detection system was implemented in Matlab v8.3 (The Mathworks Inc.). An easy-to use graphical user interface was designed, which allows to visualize and scroll through the LFP recording. Automated analysis of the LFP data can be performed one by one or in batch mode. The user can select the appropriate classifier (e.g. for chemical or genetic model) and specify the $\tau_{NLEO}$ and $\tau_{len}$ thresholds.

The analysis of the test datasets was performed in batch mode, and lasted 319 seconds (30 recordings) and 424 seconds (40 recordings) for the chemical and genetic datasets, respectively, on a computer with Intel i7-4790 3.6GHz CPU with 16GB RAM running a 64-bit Windows 7 operating system.

Upon the publication of the article we will release the software as a freeware for non-commercial use.

## 4. Discussion

We proposed an automated method to support or substitute manual analysis of zebrafish LFPs. To our knowledge, this is the first time that an LFP-based seizure detection algorithm for zebrafish is presented in detail and evaluated objectively based on independent training and test datasets.

The strength of our algorithm is its flexibility, since it can be used under different experimental conditions, such as different recording equipment or different models of epilepsy. The proposed architecture of the algorithm, i.e.

selection of candidate events, feature extraction and a machine-learning-based classification ensures a general applicability. Tuning the parameters $\tau_{NLEO}$ and $\tau_{len}$ at the event selection stage may be necessary to adjust the sensitivity of detection algorithm. For example, in a genetic model that exhibits long but low-amplitude seizures, it may be useful to lower the $\tau_{NLEO}$ parameter and increase the $\tau_{len}$ parameter. Note that tuning these parameters a-posteriori is a manual task and is not completely objective. However, it is still more objective and time-saving compared to an entirely manual analysis. On the other hand, when major differences in the seizure pattern or the typical artifact characteristics are expected, or the investigator needs to be fully blinded to the test data, it may be necessary to train a new classifier. After collecting new training data, the proposed feature extraction and machine learning approach trains the seizure detector automatically.

Indeed, we showed that the automated method reliably reproduces manual analysis and can detect significant differences between a test and control group of chemical or genetic models of epilepsy in zebrafish larvae, in terms of number of seizing larvae, and number of seizures per larvae. We demonstrated that after retrospective tuning of a single parameter, significant group differences can also be revealed by the algorithm in terms of cumulative distribution of the events. Subjective assessments have shown that using the seizure detection system in a semi-automatic way (visually validating all detections), fifteen 10 minute recordings can be analyzed in one hour, as opposed to three recordings per hour without the aid of the system. This amounts to a five-fold reduction of the workload for the LFP experts. Using the system in a fully automated way (accepting all detections without visual confirmation) is actually much faster. Depending on the chosen threshold and the number of candidate events, the system can analyze a single 10 minute recording in just a few seconds.

Moreover, we showed that the performance of our approach is in line with state-of-the-art seizure detection approaches developed and tested in rodent models of epilepsy. There is always a trade-off between the number of correctly detected events, missed events and false detections. Accordingly, our approach outperformed those in the literature in terms of some measures at the cost of others. More specifically, although we reached a relatively low sensitivity, our specificity, positive predictive value and accuracy were considerably better. This is not surprising, as we selected the optimal parameters and classifier according to the PPV. We chose this parameter as our objective was to be able to differentiate between two groups of larvae, where only one group is expected to have seizures. Therefore, in our case it was important to combine a high number of true positives along with a low number of false positives, which is quantified exactly by the PPV. Unfortunately, many studies report only specificity or accuracy, and not PPV. In two recent review articles [9] [10], accuracy was the only comparison metric among various seizure detection approaches, while in a third one [8] less than half of the methods reported a metric of false detection rate. However, in highly unbalanced classification tasks, such as seizure detection (seizures make up 1-5% of all data), a seemingly high specificity is maintained even in the presence of many false positives. Counting with 1% or 5% seizure data, and equal number of false positives and true positives as real seizures (in which case there is 50% chance that a detected event is false), the

specificity amounts to 98.9% and 94.7%, respectively, and even higher accuracy. Clearly, although the accuracy and specificity appear to be high, the number of false positives is not acceptable, as we can have no confidence whatsoever that a detected event is truly a seizure. Therefore, we argue that precision should be always reported besides specificity and accuracy.

Nevertheless, there may be situations where false detections are less problematic, and sensitivity is crucial. For example, the seizure detection system may be used in a semi-automatic way to aid manual analysis, where LFP expert has to go through the automatically annotated recordings to exclude false events. Our proposed system could be adapted for this task as well, by tuning the parameters and training the classifier for maximal sensitivity instead of PPV in Step 5.

We used single-channel LFP recordings equipment to collect our data, therefore, our seizure detection algorithm currently works on single-channel data. However, recent technological advances allow multi-channel recordings as well [16]. Our method can easily be extended to multi-channel recordings, by simply running the method on each electrode separately, and then merging the decisions by e.g. majority voting (i.e. accept a detection if it occurs on more than half of the channels), minimum or maximum score. This strategy is called late integration. Alternatively, all features extracted from the multiple channels can be concatenated into one long feature vector, which can be used to train a single classifier. This strategy is called late integration [27] In case we can expect that the seizure pattern has the same distribution over the channels in consecutive seizures, more sophisticated integration strategies can be followed, which incorporate such spatial information [13].

Our study has a few limitations as well. The cumulative duration of seizures detected manually and automatically was significantly different in case of the chemical and genetic model. This is explained by the fact that the classifiers were not optimized for the length of the events, only for the number of events. In order to correctly retrieve the full length of seizures (without retrospective tuning, which is possible with the current algorithm as well, see section 3.3.3 and Fig. 8), another training strategy should be followed.

For practical reasons, we had to use two different LFP recording systems for our study. In a-priori subjective assessment the LFP experts found that the non-invasive equipment provided better signal quality. Indeed, we have achieved good detection performance for both non-invasively recorded test sets. It is interesting to note that the algorithm achieved a reasonable performance for the genetic model recorded non-invasively as well, even though, and as a matter of fact, an inferior quality invasive system was used to record the training set.

In summary, we presented a generic seizure detection system that produces reliable results. We conclude that it can aid or even replace manual analysis, saving time and rendering zebrafish LFP analysis more objective, facilitating epilepsy and drug discovery research.

**Acknowledgements**

B.H was financially supported by the following agencies: iMinds Medical Information Technologies; Dotatie-Strategisch basis onderzoek (SBO- 2016); European Research Council: The research leading to these results has received funding from the European Research Council under the European Union's Seventh Framework Programme (FP7/2007-2013) / ERC Advanced

Grant: BIOTENSORS (n° 339804). This paper reflects only the authors' views and the Union is not liable for any use that may be made of the contained information.
A. S. is a postdoctoral fellow of the Research Foundation–Flanders (FWO Vlaanderen). This project was carried out with the support of the Agency for Innovation by Science and Technology (project nr 131179, IWT, Flanders).

## References

1] J. Engel, "Surgery for seizures," *New ngland Journal of Medicine,* vol. 334, pp. 647-653, 1996.

2] D. J. Thurman, E. Beghi, C. E. Begley, A. T. Berg, J. R. Buchhalter, D. Ding, D. C. Hesdorffer, W. A. Hauser, L. Kazis, R. Kobau, B. Kroner, D. Labiner, K. Liow, G. Logroscino and M. T. Medina, "Standards for epidemiologic studies and surveillance of epilepsy," *Epilepsia,* vol. 52, no. s7, pp. 2-26, 2011.

3] S. Berghmans, J. Hunt, A. Roach and P. Goldsmith, "Zebrafish offer the potential for a primary screen to identify a wide variety of potential anticonvulsants," *Epilepsy Research,* vol. 75, pp. 18-28, 2007.

4] G. A. Hortopan, M. T. Dinday and S. C. Baraban, "Zebrafish as a model for studying genetic aspects of epilepsy," *Dis Models Mech,* vol. 3, pp. 144--, 2010.

5] D.-H. Pham, B. Hunyadi, L. Moons and P. de Witte, "A zebrafish model of epileptogenesis and refractory epilepsy induced by kainic acid," vol. submitted, pp. --, 2016.

6] V. K. Jirsa, W. C. Stacey, P. P. Quilichini, A. I. Ivanov and C. Bernard, "On the nature of seizure dynamics," *Brain,* vol. 137, pp. 2210--, 2014.

7] J. Gotman, "Automatic recognition of epileptic seizures in the EEG," *Electroencephalography and clinical Neurophysiology ,* vol. 54, no. 5, pp. 530-540., 1982.

8] T. N. Alotaiby, S. A. Alshebeili, T. Alshawi, I. Ahmad and F. E. Abd El-Samie, "EEG seizure detection and prediction algorithms: a survey," *EURASIP Journal on Advances in Signal Processing ,* vol. 2014, no. 1, p. 183, 2014.

9] U. R. Acharya, S. V. Sree, G. S. Roshan, J. Martis and J. S. Suri, "Automated EEG analysis of epilepsy: A review,," *Knowledge-Based Systems,* vol. 45, pp. 147-165, 2013.

10] A. T. Tzallas, D. G. Tsalikakis, E. C. Karvounis, L. Astrakas, M. Tzaphlidou, M. G. Tsipouras and S. Konitsiotis, "Automated epileptic seizure detection methods: a review study.," INTECH Open Access Publisher, 2012.

11] F. Fürbass, M. Hartmann, H. Perko, A. Skupch, P. Dollfuss, G. Gritsch, G. B. C. Gritsch and T. Kluge, "Combining time series and frequency domain analysis for a automatic seizure detection.," in *Annual International Conference of the IEEE Engineering in Medicine and Biology Society EMBC*, San Diego, 2012 .

12] W. Deburchgraeve, P. Cherian, M. De Vos, S. R.M., B. J.H., G. Visser, P. Govaert and S. an Huffel, "Automated neonatal seizure detection mimicking

a human observer reading EEG," *Clinical Neurophysiology,* vol. 119, p. 2447–2454, 2008.

13] B. Hunyadi, M. Signoretto, W. Van Paesschen, J. Suykens, S. Van Huffel and M. De Vos, "Incorporating structural information from the multichannel EEG improves patient-specific seizure detection," *Clinical Neurophysiology,* vol. 123, no. 12, pp. 2352-2361, 2012.

14] R. A. Bergstrom, J. H. Choi, A. Manduca, H.-S. Shin, G. A. Worrell and C. L. Howe, "Automated identification of multiple seizure-related and interictal epileptiform event types in the EEG of mice," *Scientific reports,* vol. 3, pp. 1483--, 2013.

15] F. Amal, G. F. Boudreaux-Bartels and W. Besio, "Automatic seizure detection in rats using Laplacian EEG and verification with human seizure signals," *Annals of biomedical engineering,* vol. 41, no. 3, pp. 645-654, 2013.

16] S. Hong, P. Lee, S. C. Baraban and L. P. Lee, "A Novel Long-term, Multi-Channel and Non-invasive Electrophysiology Platform for Zebrafish," *Scientific Reports,* vol. 6, pp. 28248--, 2016.

17] S. I. d. W. P. L. L. Sourbron Jo, "Pharmacological Analysis of the Anti-epileptic Mechanisms of Fenfluramine in scn1a Mutant Zebrafish," *Frontiers in Pharmacology,* vol. 8, p. 191, 2017.

18] J. Schubert, A. Siekierska, M. Langlois, P. May, C. Huneau, F. Becker, H. Muhle, A. Suls, J. Lemke, C. De Kovel and H. Thiele, "Mutations in STX1B, encoding a presynaptic protein, cause fever-associated epilepsy syndromes," *Nature Genetics,* vol. 46, no. 12, pp. 1327-1332, 2014.

19] J. Sourbron, H. Schneider, A. Kecskés, Y. Liu, E. M. Buening, L. Lagae, I. Smolders and P. de Witte, "Serotonergic Modulation as Effective Treatment for Dravet Syndrome in a Zebrafish Mutant Model," *ACS chemical neuroscience,* vol. 7, no. 5, pp. 588-598, 2016.

20] A. A. Zdebik, F. Mahmood, H. C. Stanescu, R. Kleta, D. Bockenhauer and C. Russell, "Epilepsy in kcnj10 morphant zebrafish assessed with a novel method for long-term EEG recordings," *PloS one,* vol. 8, no. 11, p. e79765, 2013.

21] T. Cover and P. Hart, "Nearest neighbor pattern classification," *IEEE transactions on information theory ,* vol. 13, pp. 21-27, 1967.

22] B. Schölkopf and A. J. Smola, Learning with kernels: support vector machines, regularization, optimization, and beyond., MIT press, 2002.

23] J. A. Suykens and J. Vandewalle, "Least squares support vector machine classifiers," *Neural processing letters,* vol. 9, pp. 293-300, 1999 .

24] P. Buteneers, D. Verstraeten, B. Van Nieuwenhuyse, D. Stroobandt, R. Raedt, K. Vonck, P. Boon and B. Schrauwen, "Real-time detection of epileptic seizures in animal models using reservoir computing," *Epilepsy Research,* vol. 103, no. 2-3, pp. 124-134, 2013.

25] G. van Luijtelaar, A. Lüttjohann, V. V. Makarov, V. A. Maksimenko, A. A. Koronovskii and A. E. Hramov, "Methods of automated absence seizure detection, interference by stimulation, and possibilities for prediction in genetic absence models," *Journal of Neuroscience Methods,* vol. 260, pp. 144-158, 2016.

M. Niknazar, S. Mousavi, S. Motaghi, A. Dehghani, B. Vosoughi Vahdat, 26] M. Shamsollahi, M. Sayyah and S. Noorbakhsh, "A unified approach for detection of induced epileptic seizures in rats using \{ECoG\} signals," *Epilepsy & Behavior,* vol. 27, no. 2, pp. 355-364, 2013.

B. R. Greene, G. B. B. Boylan, R. B. Reilly, P. de Chazal and S. Connolly, 27] "Combination of EEG and ECG for improved automatic neonatal seizure detection," vol. 118, no. 6, pp. 1348-1359, June 2007.

A. Feltane, B. Bartels, Y. Boudira and W. Besio, "Seiuzure detection 28] using empirical mode decomposition and time-frequency energy concentration," in *Signal Processing in Medicine and Biology Symposium (SPMB), 2013 IEEE*, Brooklyn, NY, 2013.